CHILEAN JOURNAL
of AGRICULTURAL RESEARCH

RESEARCH

Dynamic characteristics of leaf intracellular water, nutrients, metabolic energy, and photosynthetic responses to drought stress in maize

Melisa R. Quispe-Puma[1], Deke Xing[1*], Yanyou Wu[2*], Qian Zhang[1], and Jing Wang[1]

[1]Jiangsu University, School of Agricultural Engineering, Zhenjiang 212013, China.
[2]Chinese Academy of Sciences, State Key Laboratory of Environmental Geochemistry, Institute of Geochemistry, Guiyang 550081, China.
*Corresponding authors (wuyanyou@mail.gyig.ac.cn; xingdeke@ujs.edu.cn)

Received: 18 March 2025; Accepted: 31 May 2025, doi:10.4067/S0718-58392025000500677

ABSTRACT

Drought stress poses a major challenge to global agriculture, significantly impacting crop growth, photosynthesis, and metabolic processes. This study introduces an innovative electrophysiological approach to assess 'Xinnuo 628' sweet glutinous maize (*Zea mays* L. var. *ceratina*) responses to drought stress by integrating intracellular water, nutrient transport, and energy dynamics. The experiment was conducted in a controlled greenhouse environment with three water regimes: Control (CK, 75% field capacity), moderate drought (T1, 55%), and severe drought (T2, 35%) over 18 d. The results highlight a critical physiological inflection point on day 9 in T1, suggesting that timely irrigation at this stage could prevent irreversible damage. Under severe drought (T2), the net photosynthetic rate (P_N) dropped to 3.8 ± 0.9 $\mu mol \cdot m^{-2} \cdot s^{-1}$, and stomatal conductance (g_s) decreased to 0.09 ± 0.02 $mmol \cdot m^{-2} \cdot s^{-1}$. In contrast, T1 plants maintained a higher leaf intracellular water-holding capacity (LIWHC: 2701.34 ± 122.69) and metabolic energy reserves (ΔG_B: 356.73 ± 40.28 at day 18), enabling prolonged physiological activity despite water limitations. Electrophysiological parameters proved to be more sensitive and representative than traditional photosynthetic indicators. While LIWHC and intracellular water-use efficiency declined more gradually in T1 than in T2, photosynthetic parameters fluctuated inconsistently, especially in T2, where P_N unexpectedly increased on day 18. These findings demonstrate that electrophysiology provides a real-time, non-invasive tool to detect early stress signals and enable precise irrigation adjustments before irreversible damage occurs. By identifying the critical transition phase in T1, this study lays the basis for optimizing water use efficiency and improving maize resilience under drought conditions, contributing to the advancement of precision agriculture.

Key words: Dynamics, electrophysiology, growth, intracellular water and nutrients, water-use efficiency, *Zea mays*.

INTRODUCTION

The productivity of plants depends on it being able to grow, develop, and adapt to environmental stresses such as drought, one of the most critical issues for global agriculture (Hoseini and Arzani, 2023). It is expected that by the year 2050, freshwater availability will decrease by 50%, while water demand in agriculture will double, intensifying the pressure on agricultural systems (Farooq et al., 2024). These projections continue to be made the global need for advanced strategies that optimize water use, improve crop productivity, and ensure agricultural sustainability in the context of climate change (Zhang et al., 2019; 2020a; Burak, 2023; Ocwa et al., 2024). Even brief but intense drought events can cause significant damage, reinforcing the importance of addressing this issue with the help of new and improved strategies technologies (Black, 2024).

Maize (*Zea mays* L.), the second most widely cultivated crop in the world after wheat, is an important crop for food security due to its adaptability and resource efficiency (Erenstein et al., 2022). However, drought results in detrimental effects on productivity, as they proceed to negatively impacts the processes of photosynthesis, metabolism, and yield production (Kambona et al., 2023). Although maize has developed natural mechanisms such as stomatal regulation to mitigate water damage (Cao et al., 2021), the critical stages of its development, such as the vegetative and reproductive phases, are especially vulnerable to severe water deficits, which can drastically reduce yield (Hou et al., 2020; Li et al., 2023). These challenges once more emphasize the need for innovative strategies that adapt to both the characteristics of the crop and the environmental conditions (Liu et al., 2021).

Traditionally, plants' water needs have been assessed using indirect physiological indicators such as photosynthesis, chlorophyll content, leaf water content, and proline levels (Sun et al., 2020; Rojas-Pirela et al., 2024). Although technological advances such as moisture sensors, remote sensing, and drones have improved external monitoring of environmental factors (Song et al., 2021; Wu, 2023), these methods do not capture the intracellular dynamics of water and nutrients, which are essential for understanding responses to water stress. As we known, net photosynthetic rate does not always show a linear relationship with the leaf water content, this makes the method for diagnosing plants' water needs based on leaf water content lack precision. Besides, transpiration water can be regulated by the leaf intracellular water, and further change the photosynthesis of plants. Earlier research has shown that changes to intracellular water status affect key processes such as transcriptomes, proteomes, and hormonal levels, which are critical for lowering the slowing of photosynthesis and acting as a mechanism for plant adaptation (Niu et al., 2024; Sáez-Cigarruista et al., 2024). The leaf intracellular water demonstrates a closer and more direct relationship with photosynthesis, growth and other metabolisms of plants.

In the current context, the dynamic analysis of intracellular water and nutrient transport emerges as a promising approach. Electrophysiological techniques allow for rapid, non-invasive, and highly sensitive measurements of water status and nutrient dynamics, overcoming the limitations of traditional methods (Zhang et al., 2020b; 2021). Electrical parameters such as capacitance and impedance provide all of the real-time data on leaf water content and sap composition (Wei et al., 2024) and the changes in nutrient dynamics, revealing how plants alter their water stress responses (Qin et al., 2022). This approach is highly beneficial in that it fills in the current gaps in understanding plant water relations as well as laying the preliminary grounds for practical detection and measurement techniques for use in precision agriculture (Zhao et al., 2024).

This study introduces an innovative approach utilizing electrophysiology to assess the physiological indicators of maize under drought stress accurately and in real time. Unlike traditional methods such as photosynthesis, which can be affected by external factors and may not reflect internal dynamics, electrophysiology enables the direct measurement of intracellular water and nutrient transport. Previous research has delved into the response patterns of intracellular water, following a period of drought treatment. Additionally, some studies have examined how plant water status responds as soil moisture steadily declines during progressive drought after water supply cessation. The experiment in this current research; however, takes a different approach. By maintaining a constant drought-stress level, it aims to investigate the dynamic responses of intracellular water and nutrient transport, and other parameters of maize over time at a specific drought intensity. Based on this, it allows for a better understanding of the dynamic responses of maize plants to prolonged drought and accurate acquisition of water requirement information. This methodology significantly enhances the development of customized irrigation strategies to maximize water-use efficiency. Ultimately, it promotes the resilience of maize to drought stress and supports sustainable agricultural practices in response to the increasing global scarcity of water resources.

MATERIALS AND METHODS

Plant material, growth conditions, and experimental site

The study was conducted in a greenhouse at the Institute of Agricultural Engineering of Jiangsu University (32.11° N, 119.27° E), Jiangsu Province, China. The greenhouse is located within a subtropical monsoon climate zone. The 'Xinnuo 628' seeds, a cultivar of sweet glutinous maize (*Zea mays* L. var. *ceratina*), were chosen as the experimental material for this study. 'Xinnuo 628' is a hybrid glutinous maize with yellow waxy kernels and no amylose. It was developed by crossing 'Huangnuo 337' and 'Huangnuo 312'. This cultivar is moderately sensitive to water stress during reproduction and has high disease susceptibility, which may worsen in dry conditions. Before transplantation, the seedlings underwent a 20 d pre-cultivation period in the laboratory, then were transplanted into pots (23.5 cm diameter × 24.9 cm height, approximately 11 L volume, and weighing 0.20 kg) filled with dry clay soil. Each pot rested on a 23 cm diameter and 0.06 kg plastic tray to collect drainage and reduce evaporation.

Water regimes and treatments

After transplantation, the plants underwent a 1 mo growth period before initiating measurements. The clay soil used in this study had a field capacity of 35.40%, a pH of 7.39, and a bulk density of 1.24 g cm^{-3}. It contained 10.49 g kg^{-1} organic matter, along with 56.40 mg kg^{-1} available N, 26.38 mg kg^{-1} P, and 90.40 mg kg^{-1} K, providing adequate conditions for plant growth. For the experiment, three different levels of soil relative water content (SWC_R) that will be used for treatment were established: 75% for the control (CK), 55% for moderate drought (T1), and 35% for severe drought (T2). The calculation process involved the following steps (Xing et al., 2024): (a) The soil volume in each pot was first calculated based on the soil weight and density; (b) soil water content for each treatment was calculated as the product of the SWC_R (75%, 55%, or 35%) and the soil's field capacity; (c) the amount of water needed for each treatment was then determined by multiplying the soil volume by the calculated soil water content for each SWC_R level; and (d) to maintain the specified SWC_R levels throughout the experiment, each pot was weighed regularly and adjusted daily to ensure that the soil moisture content remained consistent with the respective treatment levels.

A total of 200 seedlings were raised in the same nursery conditions. After 20 d, 60 plants were selected that looked similar in height, leaf number, and health to reduce differences among them. Then divided these plants into three groups based on different soil-water treatments (CK, T1, T2). The 18 plants were allocated to treatments in a completely randomized design with six biological replicates per treatment (n = 6). Over an 18 d experimental period, water was administered daily to both control and treated plants, and the weight of each pot containing a plant at each treatment level was consistently maintained throughout the entire treatment period.

Measurement of growth parameters

Throughout the 18 d experiment, plant growth progress was recorded. This process involves measuring stem height, stem width, and leaf length. To measure plant height and leaf length, we utilized a tapeline in centimeters, and stem diameter was evaluated using a vernier caliper in millimeters. The calculation of increases and growth speed parameters was conducted according to the following formulas:

Increase in growth parameters. The increase (ΔX) was calculated at two specific points of the experiment: Halfway through the experimental period (D9) and at the end (D18). It was determined as the difference between the measured parameter value on a specific day (X_{Dn}), and its initial value depends on the specific point (X_0):

$$\Delta X_{Dn} = X_{Dn} - X_0 \qquad (1)$$

where X is the growth parameter (length of leaf, height, and diameter of the stem), X_{Dn} is the value of the growth index on day n (D9 or D18), and X_0 is the initial value of the growth index on day 0 or day 9.

Rate of growth of the parameters. The rate of growth (GS_{Dn}) of each parameter was calculated by dividing the increase (ΔX_{Dn}) by the number of days elapsed since the start of the experiment:

$$GS_{Dn} = \Delta X_{Dn}/n \qquad (2)$$

where X is the growth parameter (length of leaf, height, and diameter of the stem), GS_{Dn} is the growth speed on day n (D9 or D18), ΔX_{Dn} is the increase of the growth parameter on day n, and n is the number of days elapsed since the start of the experiment.

Measurement of photosynthetic parameters

The portable photosynthetic measurement system (Li6400XT, Li-COR, Lincoln, Nebraska, USA) was used to measure the following parameters: Net photosynthetic rate (P_N, µmol m^{-2} s^{-1}), stomatal conductance (g_s, mmol m^{-2} s^{-1}), and transpiration rate (E, mmol m^{-2} s^{-1}). The instantaneous water use efficiency (WUE_i, mol $mmol^{-1}$) was calculated according to the following equation:

$$WUE_i = P_N/E \qquad (3)$$

The measurements were conducted between 08:30 and 10:30 h on days 0, 9, and 18 under sunny conditions, using natural light as the source. The third leaf from the top of the plant was consistently chosen for all determinations to ensure uniformity in the data collection process.

Measurement of electrophysiological parameters

During the experiment, we used a LCR tester (LCR HiTESTER 3532-50, HIOKI, Nagano, Japan) to record the electrophysiological parameters by the procedure described by Xing et al. (2022). We selected three different sites on each leaf to record the electrophysiological parameters. Data were collected on days 0, 9, and 18. We used a 10 mm diameter electrode plate with a measuring voltage of 1.5 V and a frequency of 3000 Hz. We added iron blocks to adjust the device's pressure, weighing 0.1 kg (N).

The coupling models of gripping force and electrophysiological parameters are calculated according to the Nerst equation and Energy Conservation law. Then, the leaf intracellular water-holding capacity (LIWHC), leaf intracellular water-use efficiency (LIWUE), leaf intracellular water holding time (LIWHT) and leaf intracellular water transport rate (LIWTR) (Zhang et al., 2020b) can be calculated. The formulas were as follows, described by Wang et al. (2024):

$$\mathrm{LIWHC} = \sqrt{(\mathrm{IC_p})^3} \qquad (4)$$

$$\mathrm{LIWUE} = \frac{\mathrm{d}}{\mathrm{LIWHC}} \qquad (5)$$

$$\mathrm{LIWHT} = \mathrm{IC_p} \times \mathrm{IZ} \qquad (6)$$

$$\mathrm{LIWTR} = \frac{\sqrt{(\mathrm{IC_p})^3}}{\mathrm{IC} \times \mathrm{IZ}} \qquad (7)$$

where IC_p (pF) is the leaf's physiological capacitance, IZ is the intrinsic impedance of the plant leaf (MΩ), and d is the specific effective thickness of the leaf.

According to Wang et al. (2024), this study employs formulas for active and passive nutrient transport (NAT and NPT), nutrient tolerance (RLN%), and nutrient use efficiency (NUE) of plants based on electrophysiological parameters:

$$NAT = \frac{IR}{IXL} \qquad (8)$$

$$NPT = \frac{IR}{IXc} \qquad (9)$$

$$RLN = \frac{100 \times NAT}{NAT + NPT} \qquad (10)$$

$$NUE = \frac{100}{NAT + NPT} \qquad (11)$$

The following methods and formulas were applied to calculate the physiological parameters related to plant cellular metabolic energy (Deng et al., 2021; Chen et al., 2022):

Cellular metabolic energy based on physiological impedance (ΔG_Z)

$$\Delta G_Z = \Delta G_{Z-E} \times d \qquad (12)$$

Cellular metabolic energy based on physiological resistance (ΔG_R)

$$\Delta G_R = \Delta G_{R-E} \times d \qquad (13)$$

Overall cellular metabolic energy (ΔG_B)

$$\Delta G_B = \frac{\Delta G_Z + \Delta G_R}{2} \qquad (14)$$

where ΔG_{Z-E} is unit metabolic energy of plant leaf cells based on physiological impedance and ΔG_{R-E} is unit metabolic energy of plant cells based on physiological resistance, they are the unit metabolic energy of plant leaf cells based on physiological resistance and reactance, respectively, and d is the specific effective thickness of the leaf.

And, to calculate the relative metabolic activity (MA):

$$MA = (MF \times MR)^{1/6} \qquad (15)$$

where MF is the leaf metabolic flux and MR is the leaf metabolic rate. Measuring the electrical properties of leaves provides a quick and non-invasive way to understand the water and metabolic condition of plant cells.

Statistical analysis

The valid data was obtained using Microsoft Excel 2019. SigmaPlot software (version 14.0, Graffiti, Palo Alto, California, USA) fits the electrophysiological parameter curves. The SPSS software was used for statistical analysis (version 25.0, IBM, Armonk, New York, USA). Duncan's multiple comparison tests and a one-way ANOVA at the 0.05 significance level were used to evaluate the differences among the experimental treatments. The visual representation of the data was created using the OriginPro 2024b graphing tool (Learning edition, OriginLab Corporation, Northampton, Massachusetts, USA).

RESULTS

Effects of drought on growth parameters

The results show how different levels of water stress (CK, T1, T2) significantly affect the growth parameters of maize, including leaf length (L), height (H), and stem diameter (D) (Table 1). Measuring the growth parameters of the maize plant is crucial for early detection of abnormalities; furthermore, it helps optimize resources to maximize crop yield (Zhao et al., 2024). During the experimental period, different responses were observed in the growth index (ΔL, ΔH, ΔD) and growth speed (GS) based on the drought treatments. Table 1 summarizes these variations at two key points: Halfway through the experiment (D9) and at the end of the experiment (D18).

Table 1. Growth parameters of maize under drought stress. Mean ± SE (n = 5) followed by different letters in the same column significantly differ at $P < 0.05$ according to one-way ANOVA. SWC_R: Soil relative water content; T: treatment; CK: 75% field capacity for the control; T1: 55% field capacity for moderate drought; T2: 35% field capacity for severe drought; D: day; ΔL: increase in leaf length (cm); ΔH: increase in stem height (cm); ΔD: increase in stem diameter (mm); GS: growth speed.

SWC_R		Length leaf		Height		Diameter	
T	D	ΔL	GS	ΔH	GS	ΔD	GS
		cm	cm d^{-1}	cm	cm d^{-1}	mm	mm d^{-1}
CK	D9	3.62 ± 0.66^{a}	0.39 ± 0.07^{a}	3.34 ± 0.55^{a}	0.37 ± 0.06^{a}	5.49 ± 1.12^{a}	0.60 ± 0.12^{a}
	D18	3.60 ± 0.61^{a}	0.40 ± 0.06^{a}	2.26 ± 0.48^{a}	0.25 ± 0.05^{a}	3.51 ± 0.28^{a}	0.39 ± 0.03^{a}
T1	D9	1.48 ± 0.23^{b}	0.16 ± 0.02^{b}	2.50 ± 0.54^{a}	0.28 ± 0.06^{a}	4.66 ± 0.87^{a}	0.51 ± 0.09^{a}
	D18	1.50 ± 0.19^{b}	0.16 ± 0.02^{b}	1.20 ± 0.21^{b}	0.13 ± 0.02^{b}	3.48 ± 0.58^{a}	0.39 ± 0.06^{a}
T2	D9	1.06 ± 0.08^{b}	0.11 ± 0.00^{b}	0.78 ± 0.18^{b}	0.09 ± 0.02^{b}	1.50 ± 0.25^{b}	0.16 ± 0.02^{b}
	D18	0.80 ± 0.12^{b}	0.09 ± 0.01^{b}	0.62 ± 0.16^{b}	0.06 ± 0.01^{b}	1.81 ± 0.46^{b}	0.20 ± 0.05^{b}

The control plants (CK) showed consistent development across all parameters. At D18 they achieved the greatest leaf length (ΔL = 3.6 ± 0.61 cm) and height (ΔH = 2.26 ± 0.48 cm), maintaining the highest growth rate among all treatments. Relative to CK, T2 plants exhibited a 77.8% reduction in leaf length and a 72.6% reduction in plant height at D18 (Table 2). The diameter (ΔD) and GS of the plants in T1 showed no clear difference with those in CK. Under severe stress (T2), the plants exhibited a drastic reduction in growth compared to CK. By D18, the leaf length and stem diameter were significantly lower (ΔL = 0.8 ± 0.12 cm; ΔD = 1.81 ± 0.46 mm), with stem reduced by 48.4% and the growth speed (GS_D) by 48.7%. Plants subjected to moderate stress (T1) showed partial adaptations. At D9, the growth rate and growth index for height (ΔH = 2.5 ± 0.54 cm) and diameter (ΔD = 4.66 ± 0.87 mm) were similar to CK. However, by D18, the height significantly decreased (ΔH = 1.20 ± 0.21 cm), corresponding to a 46.9% reduction, although the stem diameter remained close to CK values (ΔD = 3.48 ± 0.58 mm), with only a 0.9% decrease.

Particularly, the diameter is directly related to resistance, transport capacity of water and nutrients, and crop yield (Zhou et al., 2023). The plants under CK reached a maximum height of 22.5 cm at D18, significantly greater than T2 (19 cm). The T1 presented intermediate values, suggesting limited adaptation capacity to water stress. At D18, the stem diameter was larger in CK and T1, while T2 had the lowest values.

These results confirm that water stress differentially impacts the growth parameters of maize, with stem diameter and height being the most affected under severe stress. The ability of plants under T1 to maintain intermediate values in some parameters indicates possible adaptation mechanisms to water deficit.

Table 2. Percentage change in maize growth parameters relative to the control (CK). Percentage changes in maize growth parameters relative to the control (CK) were measured at each treatment level (T1: moderate drought, T2: severe drought) and at two time points (D9 and D18). The values reflect the reductions or increases in leaf length (ΔL), stem height (ΔH), and stem diameter (ΔD), along with their respective growth speeds (GS). These percentages were calculated based on the CK values for each corresponding day.

SWC$_{R}$	Day	ΔL (%)	GS$_{L}$ (%)	ΔH (%)	GS$_{H}$ (%)	ΔD (%)	GS$_{D}$ (%)
T1	D9	-59.10	-59.00	-25.10	-24.30	-15.10	-15.00
T1	D18	-58.30	-60.00	-46.90	-48.00	-0.90	0.00
T2	D9	-70.70	-71.80	-76.60	-75.70	-72.70	-73.30
T2	D18	-77.80	-77.50	-72.60	-76.00	-48.40	-48.70

Effects of drought on photosynthetic parameters

During the experiment, maize photosynthetic parameters (P_N, g_s, E, and WUE_i) exhibited dynamic trends influenced by both drought stress levels and the duration of exposure.

At the beginning of the experiment (D0), all plants showed 21.84 ± 1.62 µmol m^{-2} s^{-1} (Figure 1A). Meanwhile, the middle (D9) under severe drought (T2) showed a significant reduction in P_N (11.42 ± 0.59 µmol m^{-2} s^{-1}) compared to the control group (CK, 25.49 ± 0.66 µmol m^{-2} s^{-1}) and moderate drought (T1, 20.86 ± 0.21 µmol m^{-2} s^{-1}). This difference persisted throughout the experiment. By D18, P_N still showed lower values in T1 (17.37 ± 0.3 µmol m^{-2} s^{-1}) and T2 (14.33 ± 0.34 µmol m^{-2} s^{-1}) compared to that in CK, indicating a cumulative impact of drought stress over time.

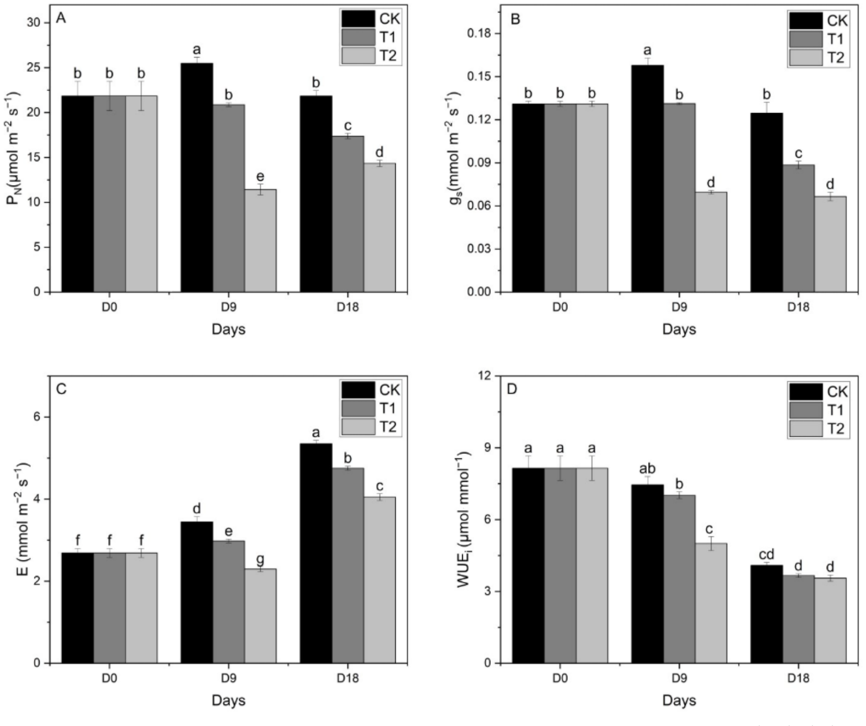

Figure 1. Photosynthetic parameters of *Zea mays*: Net photosynthetic rate (P_N) (A); stomatal conductance (g_s) (B); transpiration rate (E) (C); instantaneous water-use efficiency (WUE_i) (D). The measurement intervals were established at baseline (Day 0, D0), followed by assessments on Day 9 (D9) and Day 18 (D18). According to one-way ANOVA, different letters appear above the error when subsequent values significantly differ at $P \leq 0.05$. CK: 75% field capacity for the control; T1: 55% field capacity for moderate drought; T2: 35% field capacity for severe drought.

At D0, the g_s was 0.13 ± 0 mol m^{-2} s^{-1} (Figure 1B). Partial stomatal closure was observed in the middle of the experiment in T2, with lower g_s values on D9 (T2: 0.06 ± 0 mol m^{-2} s^{-1}) compared to CK (0.15 ± 0 mol m^{-2} s^{-1}). By D18, g_s remained lower, particularly in T1 (0.08 ± 0 mol m^{-2} s^{-1}), and T2 maintained the value (0.06 ± 0 mol m^{-2} s^{-1}).

The E values increased progressively in CK during the experiment, reaching 5.35 ± 0.08 mmol m^{-2} s^{-1} by D18 (Figure 1C). However, the increase was more limited in T1 (4.75 ± 0.04 mmol m^{-2} s^{-1}) and T2 (4.04 ± 0.08 mmol m^{-2} s^{-1}), reflecting the constraints imposed by drought stress.

At D0, the value was 8.14 ± 0.51 µmol $mmol^{-1}$ (Figure 1D). In CK and T1, WUE_i remained higher during the middle of the experiment. However, by D18, there was a significant decrease across all treatments, especially in T2 (3.55 ± 0.13 µmol $mmol^{-1}$).

A response gradient to drought stress is evident when comparing treatments at a specific time (D18). The P_N and g_s decreased drastically in T2, while T1 showed a less severe decline than CK. These results support the hypothesis that the intensity of drought directly influences the plant's ability to maintain photosynthetic processes. Thus, P_N in T1 (17.37 ± 0.3 µmol m^{-2} s^{-1}) was 20% lower than in CK (21.84 ± 0.59 µmol m^{-2} s^{-1}), while in T2 (14.33 ± 0.34 µmol m^{-2} s^{-1}), it was 34% lower.

Effects of drought on electrophysiological parameters

About the intracellular water transport, the study examined maize's intracellular water dynamics under varying drought stress levels (Table 3).

Leaf intracellular water-holding capacity (LIWHC) exhibited distinct temporal patterns across treatments. In the control group (CK), LIWHC remained relatively stable, fluctuating slightly but maintaining high values throughout the 18 d. On day 0, CK recorded 3765.2 ± 44.86, which decreased to 2485.32 ± 256.48 on D9, followed by recovery to 3680.65 ± 70.09 on D18. Moderate drought conditions (T1) exhibited a noticeable decline on D9, followed by a resurgence that culminated in a peak of 2701.34 ± 122.69 by D18. Meanwhile, a severe drought (T2) resulted in noticeably reduced LIWHC values across the experiment; on D9, the value was 1343.18 ± 72.56, and by D18, it increased to 1627.71 ± 77.32, indicating the ability of the plant to maintain intracellular water.

On D9 or D18, leaf intracellular water-use efficiency (LIWUE) maintained stable as drought stress increased, and showed no clear difference with the values on D0. Besides, no clear variation was observed in the LIWUE values at each treatment as treatment time increased.

Table 3. Leaf Intracellular water transport parameters of maize under drought stress. Mean ± SE (n = 3) followed by different letters in the same column significantly differ at $P < 0.05$ according to one-way ANOVA. T: Treatment; CK: 75% field capacity for the control; T1: 55% field capacity for moderate drought; T2: 35% field capacity for severe drought; LIWHC: leaf intracellular water-holding capacity; LIWUE: leaf intracellular water-use efficiency; LIWHT: leaf intracellular water holding time; LIWTR: leaf intracellular water transport rate

Day	T	LIWHC	LIWUE	LIWHT	LIWTR
D0	CK/T1/T2	3765.20 ± 44.86^{a}	0.05 ± 0.00^{ab}	25.61 ± 1.88^{abc}	148.56 ± 10.65^{a}
D9	CK	2485.32 ± 256.48^{b}	0.05 ± 0.00^{ab}	24.43 ± 2.38^{bc}	102.89 ± 8.16^{bc}
	T1	1757.36 ± 111.90^{c}	0.07 ± 0.01^{a}	19.75 ± 1.53^{cd}	90.19 ± 7.36^{cd}
	T2	1343.18 ± 72.56^{d}	0.07 ± 0.01^{a}	18.58 ± 1.43^{d}	72.70 ± 2.24^{d}
D18	CK	3680.65 ± 70.09^{a}	0.04 ± 0.00^{b}	31.28 ± 1.27^{a}	117.97 ± 4.08^{b}
	T1	2701.34 ± 122.69^{b}	0.05 ± 0.00^{ab}	26.71 ± 1.88^{ab}	101.73 ± 5.91^{bc}
	T2	1627.71 ± 77.32^{cd}	0.06 ± 0.00^{ab}	20.10 ± 1.58^{cd}	81.98 ± 7.64^{cd}

LIWHT remained stable in the control group (CK), gradually increasing from 25.61 ± 1.88 on day 0 to 31.28 ± 1.27 on D18. Severe drought treatment (T2) showed significantly lower LIWHT values compared to CK at each stage (D9 or D18). The T2 recorded a significantly lower LIWHT value compared to CK and T1 on D18. These trends suggest that drought stress initially reduces LIWHT but triggers compensatory mechanisms over time to prolong water retention.

Leaf intracellular water transport rate (LIWTR) declined in all treatments over time, with more pronounced reductions under severe drought (T2). On D9 and D18, CK exhibited a clearly higher LIWTR than that in T2, but showed no clear difference with the values in T1.

These findings underscore the critical role of intracellular water transport in maize's response to drought stress. The observed trends highlight the limitations of severe drought on water retention and transport and suggest that prolonged stress overwhelms the plant's adaptive capacity to sustain physiological functions.

Corresponding to intracellular nutrient transport, the research studied maize's nutrient transport under varying drought stress conditions, focusing on the next parameters (Table 4). On D9 and D18, active nutrient transport (NAT) values for CK were higher (0.39 ± 0.03) compared to T2 (0.30 ± 0.02). Over time, NAT in CK increased on D18, reaching 0.49 ± 0.02. As treatment time increased, from D9 to D18, NAT values in CK and T1 increased clearly. These results indicate that severe drought stress restricted the plants' ability to transport nutrients actively.

Table 4. Nutrient transport parameters of maize under drought stress. Mean ± SE (n = 3) followed by different letters in the same column significantly differ at $P < 0.05$ according to one-way ANOVA. T: Treatment; CK: 75% field capacity for the control; T1: 55% field capacity for moderate drought; T2: 35% field capacity for severe drought; NAT: active nutrient transport; NPT: passive nutrient transport; RLN%: nutrient tolerance; NUE: nutrient use efficiency.

Day	T	NAT	NPT	RLN%	NUE
D0	CK/T1/T2	0.41 ± 0.02^{abc}	0.56 ± 0.05^{bc}	42.66 ± 0.78^{bc}	104.10 ± 7.98^{cd}
D9	CK	0.39 ± 0.03^{bc}	0.52 ± 0.06^{bcd}	43.02 ± 0.82^{abc}	113.47 ± 14.61^{bcd}
	T1	0.32 ± 0.02^{cd}	0.40 ± 0.03^{cd}	44.69 ± 0.54^{ab}	140.42 ± 11.40^{ab}
	T2	0.30 ± 0.02^{d}	0.37 ± 0.03^{d}	45.01 ± 0.45^{a}	149.31 ± 11.26^{a}
D18	CK	0.49 ± 0.02^{a}	0.73 ± 0.04^{a}	40.25 ± 0.58^{d}	82.00 ± 4.29^{d}
	T1	0.43 ± 0.03^{ab}	0.59 ± 0.06^{ab}	42.17 ± 0.73^{cd}	99.68 ± 7.98^{d}
	T2	0.33 ± 0.02^{cd}	0.41 ± 0.03^{cd}	44.51 ± 0.53^{ab}	136.65 ± 10.73^{abc}

Passive nutrient transport (NPT) followed a similar trend to NAT on D18, with the control group showing higher values than those in T2. On D9, NPT values exhibited no clear difference among treatments. As treatment time increased, from D9 to D18, NPT values in CK and T1 also increased clearly.

Nutrient tolerance (RLN) tended to increase slightly under drought conditions. On D9, RLN values showed no clear difference among treatments. By D18, RLN in CK had decreased to 40.25 ± 0.58, whereas T2 exhibited clearly higher RLN values of 44.51 ± 0.53 compared to that in CK.

Nutrient use efficiency (NUE) showed a contrasting pattern, with significantly higher values in severe drought-stressed plants compared to the control group. On D9, NUE was 113.47 ± 14.61 for CK, while T1 and T2 recorded relatively higher values of 140.42 ± 11.4 and 149.31 ± 11.26, respectively. By D18, NUE remained highest in T2 (136.65 ± 10.73), followed by T1 (99.68 ± 7.98) and CK (82.00 ± 4.29). This increase in NUE under drought stress reflects the plants' adaptation to use the available nutrients more efficiently under stressful conditions.

The results show clear changes in nutrient transport in maize under drought stress. Both NAT and NPT were reduced in drought-stressed plants compared to the control group, highlighting how drought disrupts nutrient uptake.

And finally, for cellular metabolic energy (Table 5), the analysis under drought stress revealed the changes in Gibbs free energy and relative metabolic activity (MA), highlighting the impact of water deficit on plant physiology. The main findings are detailed below:

On D9, CK had a ΔG_Z of 538.96 ± 139.99, while the moderate stress group (T1) and severe stress group (T2) showed a slightly lower value 397.55 ± 62.25 and 239.59 ± 37.85, respectively. By D18, the values kept stable compared to those on D9.

On D9, ΔG_R followed a similar trend to ΔG_Z, with the control group at 538.2 ± 136.54, the moderate group at 407.39 ± 58.37, and the severe group at 237.39 ± 37.86. By D18, nonsignificant reduction was observed in all three treatments, with the severe group showing the value (223.08 ± 13.99), while the control remained relatively high (514.43 ± 63.99).

Table 5. Cellular metabolic energy parameters of maize under drought stress. Mean ± SE (n = 3) followed by different letters in the same column significantly differ at $P < 0.05$ according to one-way ANOVA. T: Treatment; CK: 75% field capacity for the control; T1: 55% field capacity for moderate drought; T2: 35% field capacity for severe drought; ΔG_Z: cellular metabolic energy based on physiological impedance; ΔG_R: cellular metabolic energy based on physiological resistance; ΔG_B: overall cellular metabolic energy; MA: relative metabolic activity.

Day	T	ΔG_Z	ΔG_R	ΔG_B	MA
D0	CK/T1/T2	683.96 ± 133.24^{a}	676.03 ± 193.76^{a}	679.99 ± 161.70^{a}	16.49 ± 1.03^{a}
D9	CK	538.96 ± 139.99^{ab}	538.20 ± 136.54^{ab}	538.58 ± 138.20^{ab}	12.39 ± 0.78^{bc}
	T1	397.55 ± 62.25^{ab}	407.39 ± 58.37^{ab}	402.47 ± 60.14^{ab}	11.28 ± 0.73^{bcd}
	T2	239.59 ± 37.85^{b}	237.39 ± 37.86^{b}	238.49 ± 37.84^{b}	9.54 ± 0.22^{d}
D18	CK	544.01 ± 66.46^{ab}	514.43 ± 63.99^{ab}	529.21 ± 65.21^{ab}	13.48 ± 0.45^{b}
	T1	369.06 ± 35.51^{ab}	344.39 ± 47.01^{ab}	356.73 ± 40.28^{ab}	12.24 ± 0.62^{bc}
	T2	230.97 ± 14.04^{b}	223.08 ± 13.99^{b}	227.03 ± 13.71^{b}	10.46 ± 0.77^{cd}

On D9, the severe group (T2) reported a ΔG_B of 238.49 ± 37.84, relatively lower than both the control group (538.58 ± 138.20) and the moderate group (402.47 ± 60.14). By D18, the severe group had reached a critical value of 227.03 ± 13.71, while the moderate and control groups-maintained values of 356.73 ± 40.28 and 529.21 ± 65.21, respectively.

Drought stress also reduced MA, with progressive declines throughout the experiment: On D9 and D18, the value in CK was remarkably higher than that in T2, but showed no clear difference with that in T1.

The results indicate that severe drought stress significantly decreases the relative MA in maize. Plants subjected to severe stress (T2) showed lower values for MA compared to CK. This suggests a drastic reduction in the cells' ability to sustain basic metabolic functions and adapt to water deficit.

DISCUSSION

The physiological and morphological responses of maize to water stress reflect key adaptation strategies to adverse conditions. In this study, two levels of water stress (T1 and T2) were evaluated for 18 d, identifying significant differences in the plant's ability to tolerate drought. In T2 (severe stress), growth, measured in height and stem diameter, showed rapid inhibition, with critical values on day 9 (D9). The average height in T2 was 0.78 ± 0.18 cm, compared to 2.5 ± 0.54 cm in T1 and 3.34 ± 0.55 cm in the control (CK). This deterioration was accompanied by a marked decrease in net photosynthetic rate (P_N), which dropped to 3.8 ± 0.9 μmol m^{-2} s^{-1}, and in stomatal conductance (g_s), reducing to 0.09 ± 0.02 mmol m^{-2} s^{-1}. These results confirm that stomatal closure limits gas exchange, restricting photosynthesis and reducing biomass accumulation (Yasin et al., 2022).

However, when analyzing the photosynthetic parameters, certain inconsistencies were observed. On D9, T2 showed a P_N of 11.4 μmol m^{-2} s^{-1}. In comparison, on D18, this value increased to 14.3 μmol m^{-2} s^{-1}, which does not align with the progression of physiological deterioration recorded in other parameters. A possible explanation is that, under severe stress conditions, maize may activate osmotic adjustment mechanisms or resource reallocation. However, since g_s did not show an equivalent increase, this rise in P_N could be due to non-stomatal factors, such as dynamics of leaf intracellular water. These results confirm the importance of complementing the photosynthetic parameter set down with water transport and energy metabolism parameters to obtain a wide range of parameters necessary to evaluate the plant's water status.

The indicators of intracellular water (leaf intracellular water-holding capacity, leaf intracellular water holding time) reflected significantly lower retention in T2. At D18, leaf intracellular water-holding capacity (LIWHC) values decreased to 1627.71 ± 77.32, compared to 2701.34 ± 122.69 in T1. This severe deficit interrupted the relationship between intracellular water, nutrients, and photosynthetic activity, affecting essential processes such as chlorophyll synthesis and enzymatic activation (Buenrostro Rodríguez et al., 2023). Severe drought stress had a remarkable negative impact on the transport and use of intracellular nutrients at D18, but the influence of severe drought on nutrient transportation and utilization at D9 was not serious as that at the D18. Similarly, the parameters of metabolic energy, overall cellular metabolic energy (ΔG_B), cellular metabolic energy based on physiological impedance (ΔG_Z), and cellular metabolic energy based on physiological resistance (ΔG_R), reflected a progressive depletion of resources. In T2, ΔG_B decreased from 238.49 ± 37.84 at D9 to 227.03 ± 13.71 at D18, indicating that plants under severe stress prioritize resources towards water absorption and osmotic regulation at the expense of growth. This aligns with previous studies suggesting that energy metabolism is strategically redistributed in response to prolonged water stress (Yu et al., 2022).

The analysis of transpiration (E) showed unexpected patterns. At D9, E in T1 and T2 was 2.9 and 2.2 mmol $m^{-2} s^{-1}$, respectively, increasing to 4.7 and 4.0 mmol $m^{-2} s^{-1}$ at D18. Since stomatal closure is the first response to water stress, a continuous reduction in transpiration would be expected. However, its increase at D18 suggests that, in addition to stomatal control, transpiration also responds to external factors such as temperature and humidity (Griffani et al., 2024). This indicates that maize's water regulation is weak under prolonged drought conditions, affecting its water use efficiency.

Under moderate stress (T1), the plants exhibited better adaptation capacity. By D9, height (2.5 ± 0.54 cm) and stem diameter (0.51 ± 0.09 mm d^{-1}) remained close to control values. However, by D18, height stabilized at 1.2 ± 0.21 cm, while diameter reached 3.48 ± 0.58 mm, indicating better structural conservation than in T2. Water and metabolic energy indicators highlighted critical differences between T1 and T2. In T1, LIWHC partially recovered at D18 (2701.34 ± 122.69), whereas in T2, values remained critically low from D9. Similarly, ΔG_B in T1 decreased from 402.47 ± 60.14 at D9 to 356.73 ± 40.28 at D18, but not significantly, reflecting less severe energy reduction than in T2. This confirms that plants in T1 managed to sustain essential metabolic functions for longer, increasing their resilience to water stress.

This study was conducted in a controlled greenhouse using a single maize hybrid; however, key electrophysiological parameters (LIWHC and ΔG_B) are biophysically conserved and potentially applicable across genotypes. Ali et al. (2019) reported significant variation in drought responses among eight maize hybrids, supporting the relevance of physiological screening. Electrophysiological tools can detect early internal water and energy changes, facilitating selection at early growth stages when visual differences are minimal. To connect lab findings with field performance, Tao et al. (2023) developed the normalized temperature drought index (NTDI), which uses satellite-based normalized difference vegetation index (NDVI) and surface temperature to track drought and soil moisture. Integrating in-plant electrophysiological metrics with NTDI could enable a two-tiered drought monitoring system—combining plant-level stress detection with landscape-scale moisture assessment to guide genotype selection, irrigation, and early warning strategies.

The karst (*Orychophragmus violaceus* (L.) O.E. Schulz) plants have developed a suite of mechanisms through which they have developed to cope with water stress, including modifications in leaf structure, greater cellular elasticity, and more efficient translocation of intracellular water (Xing et al., 2022). In contrast, maize, which has a limited ability to regulate its water homeostasis, is more susceptible to prolonged drought conditions this indicates the need for agronomic strategies that take advantage of the use of precision instruments to enhance the resilience of maize, using advanced monitoring of water status. From an agronomic perspective, these results underline the importance of implementing precision irrigation strategies, especially before D9, to prevent irreversible damage. Tools such as electrophysiological analysis allow for assessing water demand in real-time, enabling water use efficiency and reducing crop loss in times of stress (Cattani et al., 2024).

CONCLUSIONS

This study shows that water stress significantly impacts the growth, photosynthesis, and intracellular water, nutrient, and energy dynamics in maize under severe drought (35% field capacity), plant growth parameters, photosynthetic capacity, and intracellular water retention declined sharply, suggesting limited adaptability. Growth reductions reached over 70% in some parameters, highlighting the magnitude of drought impact. In contrast, plants under moderate stress (55% field capacity) could maintain crucial processes longer, indicating adaptive mechanisms that enhance physiological resilience.

The results underscore the value of electrophysiological parameters as sensitive and reliable indicators of environmental water conditions and intracellular dynamics in real time. Although photosynthetic parameters also respond to water stress, they have limitations in capturing the prolonged effects of drought with precision and dynamism, emphasizing the importance of combining both approaches to achieve a more comprehensive evaluation of plant water status.

Electrophysiology emerges as an innovative tool for assessing water and metabolic homeostasis in crops subjected to drought, addressing gaps left by traditional methods. Its applicability across maize genotypes and potential for integration with field-scale tools. Integrating these techniques into agricultural monitoring could pave the way for more precise irrigation strategies, optimizing water use, and enhancing crop resilience to climate variability.

Finally, testing and refining these protocols across diverse agroecological zones will be key to ensuring their global relevance in sustainable agriculture.

Author contributions

Conceptualization: Y.W. Methodology: D.X., M.R.Q-P. Formal analysis: M.R.Q-P., Q.Z. Investigation: M.R.Q-P., J.W. Data curation: Y.W., D.K. Writing-original draft: M.R.Q-P. Writing-review & editing: Y.W., D.X. Supervision: Y.W., D.X. Project administration: Y.W. Funding acquisition: Y.W. All co-authors reviewed the final version and approved the manuscript before submission.

Acknowledgements

This research was funded by the National Key Research and Development Program of China (No. 2021YFD1100300), and the Priority Academic Program Development of Jiangsu Higher Education Institutions (PAPD-2023-87).

References

Ali, A., Ahmed, A., Rashid, M., Kalhoro, S.A., Maqbool, M., Ahmed, M., et al. 2019. Screening of maize (*Zea mays* L.) hybrids based on drought tolerance under hydroponic conditions. Pure and Applied Biology 8(1):625-633. doi:10.19045/bspab.2019.80002.

Black, E. 2024. Global change in agricultural flash drought over the 21st century. Advances in Atmospheric Science 41(1):209-220. doi:10.1007/s00376-023-2366-5.

Buenrostro Rodríguez, J.F., Covarrubias Prieto, J., Solís Moya, E., Ledesma Ramirez, L., González Figueroa, S.S., Mandujano Bueno, A., et al. 2023. Effect of drought stress on wheat yield, chlorophyll, and biomass. Revista Fitotecnia Mexicana 46(3):245-253. doi:10.35196/rfm.2023.3.245.

Burak, Ş. 2023. Determining the changing irrigation demands of maize production in the Cukurova Plain under climate change scenarios with the CROPWAT model. Water 15:4215. doi:10.3390/w15244215.

Cao, L., Lu, X., Wang, G., Zhang, P., Fu, J., Wang, Z., et al. 2021. Transcriptional regulatory networks in response to drought stress and rewatering in maize (*Zea mays* L.) Molecular Genetics and Genomics 296(6):1203-1219. doi:10.1007/s00438-021-01820-y.

Cattani, A., de Riedmatten, L., Roulet, J., Smit-Sadki, T., Alfonso, E., Kurenda, A., et al. 2024. Water status assessment in grapevines using plant electrophysiology. OENO One 58(4):8209. doi:10.20870/oeno-one.2024.58.4.8209.

Chen, T., Wu, Y., Xing, D., Duan, R. 2022. Effects of $NaHSO_3$ on cellular metabolic energy, photosynthesis and growth of *Iris pseudacorus* L. Horticulturae 8(2):185. doi:10.3390/horticulturae8020185.

Deng, Z., Li, C., Wu, Y. 2021. Comparison of metabolic energy in two mulberry species based on leaf electrophysiological properties. Earth and Environment 3:307-314. doi:10.14050/j.cnki.1672-9250.2021.49.063.

Erenstein, O., Jaleta, M., Sonder, K., Mottaleb, K., Prasanna, B.M. 2022. Global maize production, consumption and trade: Trends and R&D implications. Food Security 14(6):1295-1319. doi:10.1007/s12571-022-01288-7.

Farooq, M., Wahid, A., Zahra, N., Hafeez, M.B., Siddique, K.H.M. 2024. Recent advances in plant drought tolerance. Journal of Plant Growth Regulation 43:3337-3369. doi:10.1007/s00344-024-11351-6.

Griffani, D.S., Rognon, P., Farquhar, G.D. 2024. The role of thermodiffusion in transpiration. New Phytologist 243(4):1301-1311. doi:10.1111/nph.19642.

Hoseini, M., Arzani, A. 2023. Epigenetic adaptation to drought and salinity in crop plants. Journal of Plant Molecular Breeding 11(2):1-16. doi:10.22058/jpmb.2024.2021261.1292.

Hou, G., Dong, Y., Zhu, F., Zhao, Q., Chen, Y. 2020. MicroRNA transcriptomic analysis of the sixth leaf of maize (*Zea mays* L.) revealed a regulatory mechanism of jointing stage heterosis. BMC Plant Biology 20:541. doi:10.1186/s12870-020-02751-3.

Kambona, C.M., Koua, P.A., Léon, J., Ballvora, A. 2023. Stress memory and its regulation in plants experiencing recurrent drought conditions. Theoretical and Applied Genetics 136(2):26. doi:10.1007/s00122-023-04313-1.

Li, Y., Zhang, P., Sheng, W., Zhang, Z., Rose, R.J., Song, Y. 2023. Securing maize reproductive success under drought stress by harnessing CO_2 fertilization for greater productivity. Frontiers in Plant Science 14:1221095. doi:10.3389/fpls.2023.1221095.

Liu, M., Wang, G., Liang, F., Li, Q., Tian, Y., Jia, H. 2021. Optimal irrigation levels can improve maize growth, yield, and water use efficiency under drip irrigation in Northwest China. Water 14(23):3822. doi:10.3390/w14233822.

Niu, L., Wang, Y., Li, X. 2024. Maize multi-omics reveal leaf water status controlling differential transcriptomes, proteomes and hormones during osmotic stress. Plant Omics 17(3):456-467. doi:10.1007/s44154-024-00159-9.

Ocwa, A., Bojtor, C., Illés, Á., Ssemugenze, B., Balaout, I., Rátonyi, T., et al. 2024. Precision drip irrigation system and foliar application of biostimulants and fertilizers containing micronutrients optimize photochemical efficiency and grain yield of maize (*Zea mays* L.) Journal of Soil Science and Plant Nutrition 24:7786-7800. doi:10.1007/s42729-024-02074-4.

Qin, X., Xing, D., Wu, Y., Wang, W., Li, M., Solangi, K. 2022. Diurnal variation in transport and use of intracellular leaf water and related photosynthesis in three karst plants. Agronomy 12(11):2758. doi:10.3390/agronomy12112758.

Rojas-Pirela, M., Carillo, P., Lárez-Velásquez, C., Romanazzi, G. 2024. Effects of chitosan on plant growth under stress conditions: Similarities with plant growth promoting bacteria. Frontiers in Plant Science 15:1423949. doi:10.3389/fpls.2024.1423949.

Sáez-Cigarruista, J., Morales-Guevara, D., Gordon-Mendoza, R., Jaén-Villarreal, J., Franco-Barrera, J., Ramos-Manzané, F. 2024. Sensibilidad del cultivo de maíz (*Zea mays* L.) a diferentes períodos de déficit hídrico controlado. Agronomía Mesoamericana 35(1):55660. doi:10.15517/am.2024.55660.

Song, X., Zhou, G., He, Q. 2021. Critical leaf water content for maize photosynthesis under drought stress and its response to rewatering. Sustainability 13(13):7218. doi:10.3390/su13137218.

Sun, Y., Wang, C., Chen, H.Y., Ruan, H. 2020. Response of plants to water stress: A meta-analysis. Frontiers in Plant Science 11:541682. doi:10.3389/fpls.2020.00978.

Tao, L., Di, Y., Wang, Y., Ryu, D. 2023. Normalized temperature drought index (NTDI) for soil moisture monitoring using MODIS and Landsat-8 data. Remote Sensing 15(11):2830. doi:10.3390/rs15112830.

Wang, J., Su, Y., Wei, J., Zhang, Q., Huang, B., Xing, D., et al. 2024. Comparison of intrinsic electrophysiological characteristics among different varieties of three Brassicaceae crops. Seed 43(5):48-55. doi:10.16590/j.cnki.1001-4705.2024.05.048.

Wei, P., Li, H., Wu, Y., Zhang, C. 2024. Association of the electrical parameters and photosynthetic characteristics of the tea tree manifests its response to simulated karst drought. Plant Signaling & Behavior 19(1):e2359258. doi:10.1080/15592324.2024.2359258.

Wu, Y. 2023. Plant physiology under abiotic stresses: Deepening the connotation and expanding the denotation. Horticulturae 9(2):218. doi:10.3390/horticulturae9020218.

Xing, D., Wang, W., Wu, Y., Qin, X., Li, M., Chen, X., et al. 2022. Translocation and utilization mechanisms of leaf intracellular water in karst plants *Orychophragmus violaceus* (L.) O.E. Schulz and *Brassica napus* L. Horticulturae 8(11):1082. doi:10.3390/horticulturae8111082.

Xing, D., Zhang, Q., Wu, Y., Zhao, K., Wang, J., Yan, S., et al. 2024. Use of transpiration water and leaf intracellular retained water in tomato (*Solanum lycopersicum* L.) plants subjected to different water supply strategies. Scientia Horticulturae 337:113520. doi:10.1016/j.scienta.2024.113520.

Yasin, M., Ahmad, A., Khaliq, T., Habib-ur-Rahman, M., Niaz, S., Gaiser, T., et al. 2022. Climate change impact uncertainty assessment and adaptations for sustainable maize production using multi-crop and climate models. Environmental Science and Pollution Research 29:18967-18988. doi:10.1007/s11356-021-17050-z.

Yu, R., Wu, Y., Xing, D. 2022. The differential response of intracellular water metabolism derived from intrinsic electrophysiological information in *Morus alba* L. and *Broussonetia papyrifera* (L.) Vent. subjected to water shortage. Horticulturae 8(2):182. doi:10.3390/horticulturae8020182.

Zhang, C., Li, X., Yan, H., Ullah, I., Zuo, Z., Li, L., et al. 2020a. Effects of irrigation quantity and biochar on soil physical properties, growth characteristics, yield and quality of greenhouse tomato. Agricultural Water Management 241:106263. doi:10.1016/j.agwat.2020.106263.

Zhang, C., Su, Y., Wu, Y., Li, H., Zhou, Y., Xing, D. 2021. Comparison on the nutrient plunder capacity of *Orychophragmus violaceus* and *Brassica napus* L. based on electrophysiological information. Horticulturae 7:206. doi:10.3390/horticulturae7080206.

Zhang, C., Wu, Y., Su, Y., Xing, D., Dai, Y., Wu, Y., et al. 2020b. A plant's electrical parameters indicate its physiological state: A study of intracellular water metabolism. Plants 9(10):1256. doi:10.3390/plants9101256.

Zhang, Y., Yu, Z., Shi, Y., Gu, S., Zhang, Y. 2019. Effects of supplemental irrigation based on soil water content on water consumption, dry matter and yield of wheat. Chilean Journal of Agricultural Research 79:190-201. doi:10.4067/S0718-58392019000200190.

Zhao, J., Chen, S., Zhou, B., He, H., Zhao, Y., Wang, Y., et al. 2024. Multitemporal field-based maize plant height information extraction and verification using solid-state LiDAR. Agronomy 14(5):1069. doi:10.3390/agronomy14051069.

Zhou, J., Wu, Y., Chen, J., Cui, M., Gao, Y., Meng, K., et al. 2023. Maize stem contour extraction and diameter measurement based on adaptive threshold segmentation in field conditions. Agriculture 13(3):678. doi:10.3390/agriculture13030678.